GEOPHYSICAL RESEARCH LETTERS, VOL. 35, L05301, doi:10.1029/2008GL033381, 2008

Structural context of the great Sumatra-Andaman Islands earthquake

Nikolai M. Shapiro,[1] Michael H. Ritzwoller[2] and E. Robert Engdahl[2]

Received 23 January 2008; accepted 4 February 2008; published 5 March 2008.

[1] A new three-dimensional seismic model and relocated regional seismicity are used to illuminate the great Sumatra-Andaman Islands earthquake of December 26, 2004. The earthquake initiated where the incoming Indian Plate lithosphere is warmest and the dip of the Wadati-Benioff zone is least steep along the subduction zone extending from the Andaman Trench to the Java Trench. Anomalously high temperatures are observed in the supra-slab mantle wedge in the Andaman back-arc. The subducting slab is observed along the entire plate boundary to a depth of at least 200 km. These factors contribute to the location of the initiation of rupture, the strength of seismic coupling, the differential rupture properties between the northern and southern segments of the earthquake, and the cause of convergence in the Andaman segment. **Citation:** Shapiro, N. M., M. H. Ritzwoller, and E. R. Engdahl (2008), Structural context of the great Sumatra-Andaman Islands earthquake, *Geophys. Res. Lett.*, *35*, L05301, doi:10.1029/2008GL033381.

1. Introduction

[2] The 26 December 2004 Sumatra-Andaman earthquake was the third largest instrumentally observed seismic event, with a moment-magnitude of about M = 9.3 [e.g., *Stein and Okal*, 2007]. Numerous studies [e.g., *Ammon et al.*, 2005; *Banerjee et al.*, 2005; *Guilbert et al.*, 2005; *Ishii et al.*, 2005; *Lay et al.*, 2005; *Ni et al.*, 2005; *Park et al.*, 2005; *Vigny et al.*, 2005; *Stein and Okal*, 2007] have demonstrated that this earthquake ruptured an area greater than 18000 km^2 along a 1300 km boundary between the Indian Plate and the Burma Microplate. The earthquake rupture proceeded along two distinct segments with different rupture properties. The southern (Sumatran) segment is characterized by normal rupture and generated most of high-frequency seismic radiation. In contrast, the northern (Andaman-Nicobar) segment of the rupture that released about two-thirds of the total seismic moment [*Stein and Okal*, 2007] had a significant component (>50%) of slow slip [e.g., *Lay et al.*, 2005]. Another peculiar observation is that, while all previous large (M > 9) earthquakes have occurred in regions where subduction is largely perpendicular to the trench, the present-day plate models and tectonic reconstructions indicate that the oblique incidence of the Indian and Burma plates (Figure 1a) has occurred west of the Andaman Sea for at least 20 million years [e.g., *Replumaz et al.*, 2004].

[3] The characteristics of this earthquake can be partially understood in terms of surface features such as the age-variability of the incoming Indian Plate along its subducting edge (Figure 1a), the existence of active spreading in the back-arc beneath the Andaman Sea [e.g., *Ortiz and Bilham*, 2003; *Khan and Chakraborty*, 2005], and anomalously strong strain partitioning [e.g., *Socquet et al.*, 2006] in which the oblique Sumatra-Andaman subduction is accommodated by strike-slip motion released along the transform Sumatra and Andaman faults that run nearly parallel to the trench. Better understanding of the earthquake and its consequences, e.g., post-seismic regional stress re-organization [e.g., *McCloskey et al.*, 2005; *Nalbant et al.*, 2005] and relaxation, will come in part from improved models of the thermal and mechanical structure of the subducting slab and the overriding plate. To address this issue we have relocated and reviewed modern and historical seismicity and produced a new shear velocity model of the uppermost mantle constructed using broadband seismic surface waves. These results help to understand the location of the initiation of rupture and to illuminate why a great earthquake occurred at a highly oblique plate boundary and why rupture proceeds differently in the southern and northern segments of the fault.

2. Data and Methods

[4] To improve knowledge of historical seismicity, we relocated all instrumentally recorded earthquakes in the Andaman Islands region that are well constrained by teleseismic observations using well established methods [e.g., *Engdahl et al.*, 1998; *Engdahl and Villasenor*, 2002], giving special attention to focal depth. This earthquake catalog has been reviewed to be complete to magnitude 6.5 for the historical period (pre-1964) and 5.5 for the modern period with a relative location accuracy of about 15 km. Reviewing entails examining the internal consistency of the arrival time data, particularly the depth phases. Observed seismicity portrays the spatial distribution of interslab and intraslab (intermediate-depth) earthquakes in the region and the relationship of this seismicity to regional structures (Figures 2a–2c).

[5] We used information about surface wave phase [e.g., *Trampert and Woodhouse*, 1995; *Ekström et al.*, 1997] and group [e.g., *Ritzwoller and Levshin*, 1998; *Ritzwoller et al.*, 2002] speed dispersion across the region at periods ranging from 15 sec to 150 sec, to estimate a three dimensional (3-D) tomographic model of shear-wave speed in the upper mantle on a $1^\circ \times 1^\circ$ grid. The method involves surface-wave tomography based on finite-frequency sensitivity kernels [*Ritzwoller et al.*, 2002] followed by a Monte-Carlo inversion method [*Shapiro and Ritzwoller*, 2002, 2004] to estimate both shear velocity and temperature in the upper mantle. Plotted here are images of the middle of the ensemble of acceptable models for each

[1] Institut de Physique du Globe de Paris, CNRS, Paris, France.
[2] Center for Imaging the Earth's Interior, Department of Physics, University of Colorado, Boulder, Colorado, USA.

0094-8276/08/2008GL033381$05.00

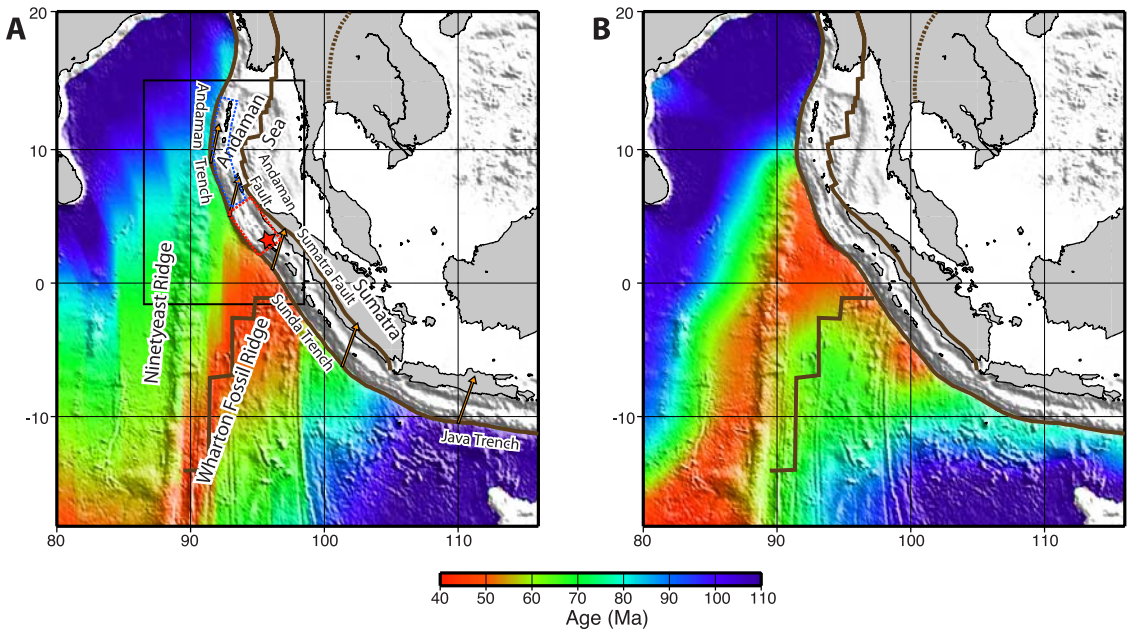

Figure 1. (a) Reference map showing the locations of the principal geographical and geological features discussed in the text. The red star marks the location of the initiation of rupture of the great Sumatra-Andaman earthquake. Brown lines show active and fossil plate boundaries. Arrows show the relative plate motion [*DeMets et al.*, 1994]. The age of the incoming oceanic plate [*Müller et al.*, 1997] is shown with colors in millions of years. The black rectangular box indicates the region shown in Figure 3. According to *Lay et al.* [2005], the large rapid slip on the southern segment of the Sumatra-Andaman earthquake (red dashed-line polygon) produced a large part of high-frequency seismic radiation while the northern segment (blue dashed-line polygon) is characterized by a significant amount of slow slip. (b) Distribution of the apparent thermal age which results from the seismic inversion using the thermal parameterization [*Ritzwoller et al.*, 2004].

variable at each depth. The temperature parameterization [*Shapiro and Ritzwoller*, 2004; *Ritzwoller et al.*, 2004] allows us to estimate the "apparent thermal age" of the oceanic lithosphere, which is the age at which a conductively cooling half-space would match the observed lithospheric temperature structure.

3. Discussion

[6] Prior to about 40 Ma, India and Australia occupied different plates separated by a spreading center called the Wharton Ridge [e.g., *Weis and Frey*, 1996; *Hébert et al.*, 1999]. After ~40 Ma, Australia rifted from Antarctica, seafloor spreading along the Wharton Ridge ceased, and India and Australia began to move in unison as part of the Australian-Indian Plate. This complex history is apparent in the variation of lithospheric age along the Andaman, Sunda, and Java Trenches (Figure 1a), with the youngest oceanic lithosphere (Wharton Fossil Spreading Ridge) of about 40 Ma currently being subducted beneath northern Sumatra [*Müller et al.*, 1997]. Significantly older lithosphere is subducting at both the Andaman and Java trenches. The seismically inferred thermal structure of the incoming Indian Plate represents the plate's tectonic history (Figure 1b). The young apparent thermal age approximately follows the Wharton Fossil Ridge with the warmest lithosphere lying somewhat to its north. The offset of the apparently youngest (and hence warmest) lithosphere from the Wharton Ridge may be explained by the influence of the Kerguelen plume [*Weis and Frey*, 1996] that delayed the thickening of the oceanic lithosphere under the Ninetyeast Ridge. The oceanic lithosphere approaching northern Sumatra (Figure 2b, profile B-B′) is also observed to be thinner than oceanic lithosphere approaching the Andaman and Java Trenches (Figures 2a and 2c), and thinner upon subduction as well.

[7] The location of the thermally warmest and thinnest incoming lithosphere is at the Sunda Trench, therefore, which nearly coincides with the initiation of rupture of the Great Sumatra-Andaman Islands earthquake and with its southern segment characterized by normal seismic rupture. This is probably no coincidence, because the warmer subducting lithosphere near the Wharton Fossil Ridge is more buoyant and the slab dips less steeply (Figure 2b). The coupling to the overlying plate, therefore, may be stronger than beneath the Andaman and Java trenches. Stronger coupling is also indicated by GPS data in this region [e.g., *Vigny et al.*, 2005]. In addition, the Benioff-Wadati zone in northern Sumatra is less steep than in adjacent areas to the north and south (30° along profile B-B′ compared with 50° and 40° along profiles A-A′ and C-C′, respectively), consistent with the thermal state of the incoming lithosphere.

[8] In the northern, subducting Andaman segment, characterized by a significant amount of "slow slip", much older and less buoyant oceanic lithosphere is subducted at the Andaman trench. The seismic velocities in the back-arc are very low in this region. This implies that the upper

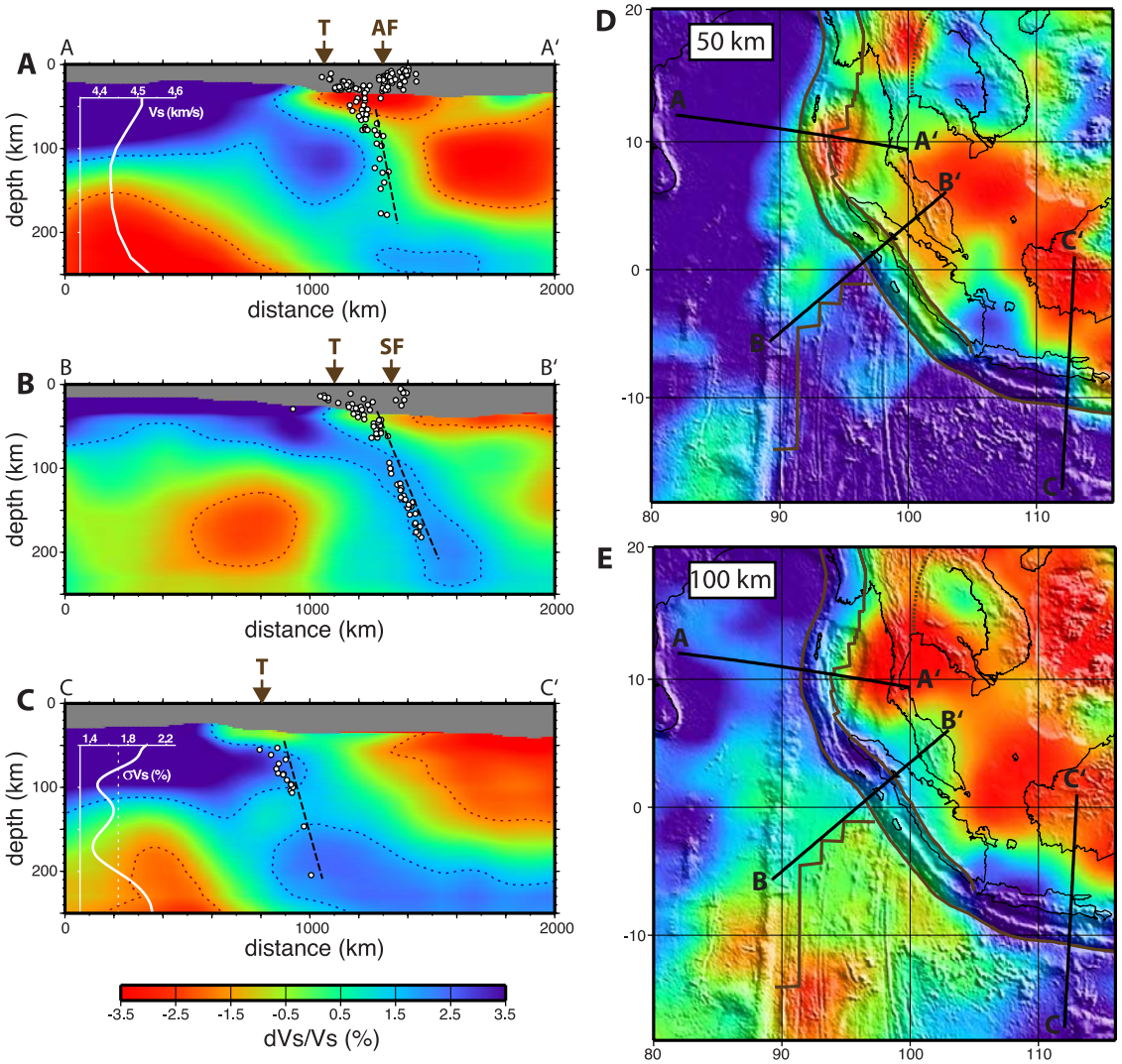

Figure 2. Results of the inversion using the seismic parameterization [*Shapiro and Ritzwoller*, 2002]. (a–c) Vertical cross-sections through the shear velocity model. Colors indicate anomalies in S-wave velocity relative to a regional one-dimensional profile shown on profile A-A′. The white line on profile C-C′ shows shear-velocity uncertainties determined during Monte-Carlo inversion [*Shapiro and Ritzwoller*, 2002]. The depth-dependent values were averaged over the region of study. Dashed contours indicate areas where positive (blue) or negative (red) Vs anomalies are stronger than 1.7% (i.e., average uncertainty for the considered depth range). The location of the trench (T) and the Sumatra (SF) and the Andaman Faults (AF) are shown with small arrows on top of the cross-sections. Hypocentres of relocated earthquakes within 100 km of the profile plane are shown by circles. Black dashed lines show the deduced orientation of the Wadati-Benioff zones. (d and e) Horizontal cross-sections through the shear velocity model at 50 km and 100 km depths, respectively.

mantle beneath the Andaman Sea is warm, consistent with its interpretation as an extensional basin created by rifting over the past 11 Ma caused by the relative motion of various lithospheric blocks in response to the collision between India and Asia [e.g., *Tapponnier et al.*, 1982; *Khan and Chakraborty*, 2005]. This combination of the less buoyant subducting plate and the weak (or rather absent) back-arc lithosphere may result in weaker seismic coupling within the Andaman segment than within the more southerly Sunda segment. This may, therefore, contribute to the differences in rupture properties and seismic radiation between these two segments of the Great Sumatra earthquake.

[9] Improved knowledge of seismicity and the thermal structure of the upper mantle also illuminates why a great earthquake occurred at a highly oblique plate boundary. Subducting lithosphere is clearly imaged by surface waves along the entire plate boundary, from the Andaman Trench to the Java trench (Figures 2a–2c and 3) down to at least 200 km depth with well defined Wadati-Benioff zones. This confirms the results from previous regional and global P-wave tomographic models [e.g., *Replumaz et al.*, 2004; *Widiyantoro and Van der Hilst*, 1996; *Hafkenscheid et al.*, 2001] and of a more recent study by *Kennett and Gummins* [2005] showing the trace of subducted oceanic lithosphere at greater depths. Centroid-moment-tensor solutions show

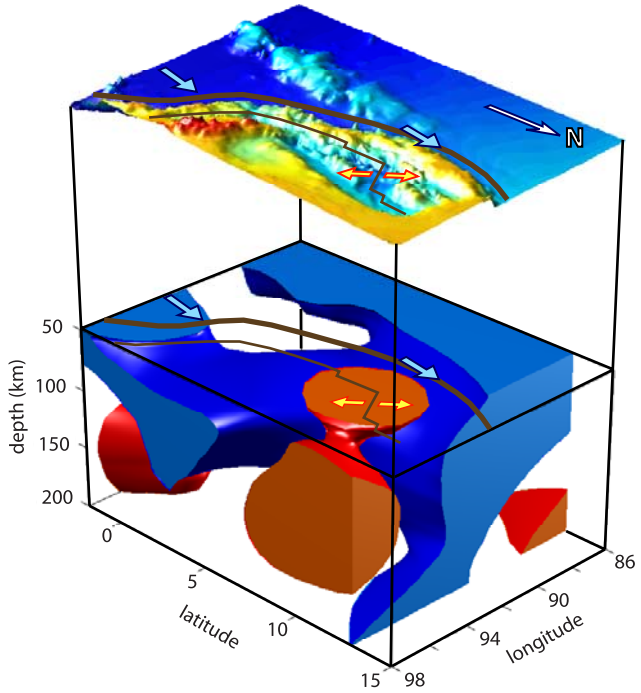

Figure 3. Isosurface representation of the shear velocity model beneath part of northern Sumatra and the Andaman Sea (identified with the black box in Figure 1), in which the model was laterally smoothed with a Gaussian filter (σ = 100 km) to highlight the dominant large-scale features. The blue surface (+1.2%) represents the high seismic velocity oceanic lithosphere subducting at the Sunda and the Andaman trenches. The gap in the blue surface corresponds to the warmest oceanic lithosphere in the vicinity of the Wharton Fossil Ridge and the Nintyeast Ridge. The red surface (−1%) reflects low seismic velocity material beneath the Andaman Sea. Vertically exaggerated topography is shown with a colored isosurface at top. The brown lines show the active plate boundaries. Blue arrows show relative plate motion and yellow arrows indicate the extension in the Andaman Basin.

that thrust earthquakes are common along the Nicobar-Andaman segment of the subduction zone with nearly east-west compression [e.g., *Rajendran and Gupta*, 1989]. Large historical (M > 8) thrust earthquakes have occurred [e.g., *Ortiz and Bilham*, 2003] along this segment and GPS data indicate non-negligible east-west convergence [*Paul et al.*, 2001]. Convergence must, therefore, be occurring and has occurred well into the past along the entire plate boundary, even beneath the most oblique Nicobar-Andaman segment of the plate boundary. This is in striking contrast with the purely transform motion observed in other very oblique segments of subduction zones. An example is the Western Aleutians [*Levin et al.*, 2005] where a "slab window" is observed beneath the trench along the highly oblique segment of the plate boundary which is devoid of both subducting lithosphere and deep seismicity. We speculate that convergence may be enhanced by the weak Andaman lithosphere responding to slab roll-back.

[10] **Acknowledgments.** The GSN [*Butler et al.*, 2004], GEOSCOPE, GEOFON, and PASSCAL data used in this work were obtained from the IRIS Data Management Center. The authors are grateful to an anonymous reviewer and Associate Editor Eric Calais for comments that helped to improve this paper and to Christophe Vigny for helpful conversations about coupling and crustal deformation in Sumatra. This work was supported by NSF grants EAR-0337622 and EAR-0409217 and by an ANR (France) contract ANR-06-CEXC-005 (COHERSIS). This is IPGP contribution 2334.

References

Ammon, C. J., et al. (2005), Rupture process of the 2004 Sumatra-Andaman earthquake, *Science*, *308*, 1133–1139.

Banerjee, P., F. F. Pollitz, and R. Bürgmann (2005), The size and duration of the Sumatra-Andaman earthquake from far-field static offsets, *Science*, *308*, 1769–1772.

Butler, R., et al. (2004), The Global Seismographic Network surpasses its design goal, *Eos Trans. AGU*, *85*(23), 225.

DeMets, C., R. G. Gordon, D. F. Argus, and S. Stein (1994), Effect of recent revisions to the geomagnetic reversal time scale on estimates of current plate motions, *Geophys. Res. Lett.*, *21*, 2191–2194.

Ekström, G., J. Tromp, and E. W. F. Larson (1997), Measurements and global models of surface waves propagation, *J. Geophys. Res.*, *102*, 8137–8157.

Engdahl, E. R., and A. Villasenor (2002), Global seismicity: 1900–1999, *International Handbook of Earthquake and Engineering Seismology*, vol. 81A, pp. 665–690, Elsevier, New York.

Engdahl, E. R., R. D. van der Hilst, and R. P. Buland (1998), Global teleseismic earthquake relocation with improved travel times and procedures for depth determination, *Bull. Seismol. Soc. Am.*, *88*, 722–743.

Guilbert, J., J. Vergoz, E. Schisselé, A. Roueff, and Y. Cansi (2005), Use of hydroacoustic and seismic arrays to observe rupture propagation and source extent of the M_w = 9.0 Sumatra earthquake, *Geophys. Res. Lett.*, *32*, L15310, doi:10.1029/2005GL022966.

Hafkenscheid, E., S. J. H. Buiter, M. J. R. Wortel, W. Spakman, and H. Bijwaard (2001), Modelling the seismic velocity structure beneath Indonesia: A comparison with tomography, *Tectonophysics*, *333*, 35–46.

Hébert, H., B. Villemant, C. Deplus, and M. Diament (1999), Contrasting geophysical and geochemical signatures of a volcano at the axis of the Wharton fossil ridge (N-E Indian Ocean), *Geophys. Res. Lett.*, *26*, 1053–1056.

Ishii, M., P. M. Shearer, H. Houston, and J. E. Vidale (2005), Extent, duration, and speed of the 2004 Sumatra-Andaman earthquake imaged by the Hi-Net array, *Nature*, *435*, 933–936.

Kennett, B. L. N., and P. R. Gummins (2005), The relationship of the seismic source and subduction zone structure for the 2004 December 26 Sumatra-Andaman earthquake, *Earth Planet. Sci. Lett.*, *239*, 1–8.

Khan, P. K., and P. P. Chakraborty (2005), Two-phase opening of Andaman Sea: A new seismotectonic insight, *Earth Planet. Sci. Lett.*, *229*, 259–271.

Lay, T., et al. (2005), The great Sumatra-Andaman earthquake of 26 December 2004, *Science*, *308*, 1127–1133.

Levin, V., N. M. Shapiro, J. Park, and M. H. Ritzwoller (2005), The slab portal beneath the Western Aleutians, *Geology*, *33*, 253–256, doi:10.1130/G20863.1.

McCloskey, J., S. S. Nalbant, and S. Steacy (2005), Indonesian earthquake: Earthquake risk from co-seismic stress, *Nature*, *434*, 291.

Müller, R. D., W. R. Roest, J.-Y. Royer, L. M. Gahagan, and J. G. Sclater (1997), Digital isochrons of the world's ocean floor, *J. Geophys. Res.*, *102*(B2), 3211–3214.

Nalbant, S. S., S. Steacy, K. Sieh, D. Natawidjaja, and J. McCloskey (2005), Earthquake risk on the Sunda trench, *Nature*, *435*, 756–757.

Ni, S., H. Kanamori, and D. Helmberger (2005), Energy radiation from the Sumatra earthquake, *Nature*, *434*, 582.

Ortiz, M., and R. Bilham (2003), Source area and rupture parameters of the 31 December 1881 M_w = 7.9 Car Nicobar earthquake estimated from tsunamis recorded in the Bay of Bengal, *J. Geophys. Res.*, *108*(B4), 2215, doi:10.1029/2002JB001941.

Park, J., et al. (2005), Earth's free oscillations excited by the 26 December 2004 Sumatra-Andaman earthquake, *Science*, *308*, 1139–1144.

Paul, J., et al. (2001), The motion and active deformation of India, *Geophys. Res. Lett.*, *28*, 647–651.

Rajendran, K., and H. K. Gupta (1989), Seismicity and tectonic stress field of a part of the Burma-Andaman-Nicobar Arc, *Bull. Seismol. Soc. Am.*, *79*, 989–1005.

Replumaz, A., H. Karason, R. D. van der Hilst, J. Besse, and P. Tapponnier (2004), 4-D evolution of SE Asia's mantle from geological reconstructions and seismic tomography, *Earth Planet. Sci. Lett.*, *221*, 103–115.

Ritzwoller, M. H., and A. L. Levshin (1998), Eurasian surface wave tomography: Group velocities, *J. Geophys. Res.*, *103*, 4839–4878.

Ritzwoller, M. H., N. M. Shapiro, M. P. Barmin, and A. L. Levshin (2002), Global surface wave diffraction tomography, *J. Geophys. Res.*, *107*(B12), 2335, doi:10.1029/2002JB001777.

Ritzwoller, M. H., N. M. Shapiro, and S. Zhong (2004), Cooling history of the Pacific lithosphere, *Earth Planet. Sci. Lett.*, *226*, 69–84, doi:10.1016/j.epsl.2004.07.032.

Shapiro, N. M., and M. H. Ritzwoller (2002), Monte-Carlo inversion for a global shear velocity model of the crust and upper mantle, *Geophys. J. Int.*, *151*, 88–105.

Shapiro, N. M., and M. H. Ritzwoller (2004), Thermodynamic constraints on seismic inversions, *Geophys. J. Int.*, *157*, 1175–1188, doi:10.1111/j.1365-246X.2004.02254.x.

Socquet, A., C. Vigny, N. Chamot-Rooke, W. Simons, C. Rangin, and B. Ambrosius (2006), India and Sunda plates motion and deformation along their boundary in Myanmar determined by GPS, *J. Geophys. Res.*, *111*, B05406, doi:10.1029/2005JB003877.

Stein, S., and E. A. Okal (2007), Ultralong period seismic study of the December 2004 Indian Ocean earthquake and implications for regional tectonics and the subduction process, *Bull. Seismol. Soc. Am.*, *97*, S279–S295, doi:10.1785/0120050617.

Tapponnier, P., G. Peltzer, A. Y. Le Dain, R. Armijo, and P. Cobbold (1982), Propagating extrusion tectonics in Asia: New insights from simple experiments with plasticine, *Geology*, *10*, 611–616.

Trampert, J., and J. H. Woodhouse (1995), Global phase velocity maps of Love and Rayleigh waves between 40 and 150 seconds, *Geophys. J. Int.*, *122*, 675–690.

Vigny, C., et al. (2005), Insight into the 2004 Sumatra-Andaman earthquake from GPS measurements in Southeast Asia, *Nature*, *436*, 201–206, doi:10.1038/nature03937.

Weis, D., and F. A. Frey (1996), Role of the Kerguelen Plume in generating the eastern Indian Ocean seafloor, *J. Geophys. Res.*, *101*, 13,831–13,849.

Widiyantoro, S., and R. D. Van der Hilst (1996), Structure and evolution of subducted lithosphere beneath the Sunda arc, Indonesia, *Science*, *271*, 1566–1570.

E. R. Engdahl and M. H. Ritzwoller, Department of Physics, University of Colorado, Campus Box 390, Boulder, CO 80309-0390, USA. (ritzwoll@ciei.colorado.edu)

N. M. Shapiro, Institut de Physique du Globe de Paris, CNRS, Box 89, 4 place Jussieu, F-75252 Paris cedex 05, France.